Research Article

Structural dependence of piezoelectric size effects and macroscopic polarization in ZnO nanowires: A first-principles study

Chuanqiong Qin, Yousong Gu (✉), Xu Sun, Xueqiang Wang, and Yue Zhang (✉)

Department of Materials Physics and Chemistry, State Key Laboratory for Advanced Metals and Materials, University of Science and Technology Beijing, Beijing 100083, China

ABSTRACT

The piezoelectric properties of [0001]-oriented ZnO nanowires are investigated via density functional theory (DFT). The axial effective piezoelectric coefficient of ZnO nanowires is significantly greater than the bulk value, and the coefficient increases as the nanowire size decreases. It is proved that the enhancement comes from both the reduction of volume per Zn–O pair and the enhancement of the Poisson's ratio. Further study shows that the macroscopic polarization behavior of ZnO nanowires is determined by the crystal structure parameters and the ratio of surface atoms, and an analytic expression is obtained. This work provides a deeper understanding of the size effects of the piezoelectricity of ZnO nanowires and sheds some light on the confusion reported on this subject.

1 Introduction

Materials with non-central-symmetry structures produce internal electrostatic potentials when subjected to external strain, which leads to piezoelectricity. Most recently, there has been an increasing interest in ZnO piezoelectric nanodevices, such as piezoelectric field-effect transistors [1], piezoelectric vibration sensors [2], and piezoelectric generators [3, 4]. The photoresponse with piezoelectricity of Cu_2O/ZnO heterojunctions [5] has also been studied since Wang introduced the concept of piezophototronics, which combines piezo-electricity and optoelectronics [6]. Piezoelectric nano-structures are distinct for three reasons: External mechanical energy is usually sufficient to actuate small piezoelectric materials [7]; it is fairly easy to prepare monocrystalline nanostructures [8, 9] that do not fail [10] with applied high strains and high electric fields; and novel properties such as quantum effects [11], interfacial effects [12], and size effects [13] become observable on a nanoscale.

On the theoretical frontier, first-principles studies

of the piezoelectricity of bulk ZnO [14] have proved to be sound, and recent studies have been very detailed about methodologies [15]. However, only a handful of theoretical investigations on ZnO nanowires have been carried out, and the obtained results are inconsistent, especially in terms of the size effect. Li et al. [16] revealed that the effective elastic constant, C_{33}, of ZnO nanowires decreases significantly with decreasing diameter, whereas the cohesive energy increases. Xiang et al. [17] reported that the effective piezoelectric coefficients of ZnO nanowires with diameters ranging from 0.6 nm to 2.8 nm are approximately 26%–39% higher than the bulk value. Agrawal and Espinosa [18] suggested significant piezoelectric size effects: Nearly 2 orders of magnitude enhancement can be attained if the diameter is reduced to less than 1 nm. However, Cicero et al. [19] and Korir et al. [20] claimed that the core region's effective piezoelectric coefficients are 1.19 C·m^{-2} and 1.21 C·m^{-2}, respectively, very close to the bulk value of 1.28 C·m^{-2} [14].

There are two causes for the above inconformity. The first one is the different definitions of the effective piezoelectric coefficient in nanowires in previous works, as the conventional definition of the piezoelectric coefficient for bulk materials is not appropriate for nanomaterials [17]. The other cause lies in the method used to calculate the volume of a nanowire, which is crucial for determining the coefficient of thin nanowires. Considering the atoms as point charges or finite spheres may result in significant difference in the volume (nearly 70% in the case of the smallest nanowires) [20], which leads to a large deviation in the coefficient depending on the dipole moment per unit volume.

In this study, density functional theory (DFT) was employed to study the piezoelectric properties of [0001]-oriented ZnO nanowires. A new method to evaluate the volume of nanowires is proposed because in previous works, the volume was a major source of confusion in the evaluation of piezoelectricity. The calculated effective piezoelectric coefficient of nanowires is found to increase as the nanowire diameter decreases, and both the average volume per Zn–O pair and the change of volume with strain are found to play key roles in the observed size effects. The structural dependence of macroscopic polarization is also studied, and it can be expressed by an analytical formula.

2 Computational methods

DFT calculations were performed using the SIESTA [21] code. A generalized gradient approximation in the form of the Perdew–Burke–Ernzerhof (GGA-PBE) exchange-correlation functional was adopted and double-ζ polarization (DZP) numerical atomic orbitals were chosen as basis sets. Norm-conserving pseudo-potentials were generated from the Troullier–Martins scheme [22] with core–valence interactions in our calculations. Mesh cutoff was 400 Ry, and the force tolerance on each atom was less than 0.02 eV·Å^{-1}. 1 × 1 × 9 Monkhorst–Pack grids were chosen after a convergence study. Piezoelectric properties were evaluated utilizing the Berry Phase [23, 24] method.

Hexagonal supercells were adopted with the same c-axes and large lateral distances between the periodic nanowires. The cross-sections of the ZnO nanowires after geometry relaxation are shown in Fig. 1(a). The samples are denoted as A, B, and C, with diameters of approximately 0.6, 1.2, and 1.8 nm, respectively.

Regarding the complicated atomic movement in a nanowire under stress, it is difficult to study the piezoelectric coefficient, e_{33}. The pragmatic effective piezoelectric coefficient, e_{33}^{eff}, is defined as reported in a previous work [18] as follows:

$$e_{33}^{\mathrm{eff}} = \partial P_3 / \partial \epsilon_3 = \partial (p_3 / V) / \partial \epsilon_3 \tag{1}$$

where P_3 and p_3 are the macroscopic polarization and dipole moment along the axial direction, respectively, and the strain, ϵ_3, is defined as the change ratio of the lattice constant, c, and V represents the volume of a certain structure. The volume occupied by a certain number of ZnO atoms in the bulk material is a well-defined quantity, and the volume of nanowires can be determined in a similar way. A rigid hexagonal ZnO nanowire can be represented as a perfect wurtzite crystal, as shown in Fig. 1(b), whereas an unrelaxed nanowire, B, is represented by a regular hexagon. The unrelaxed nanowire's constitutive volume per supercell can be defined as

$$V = Sc \tag{2}$$

where S is the cross-sectional area and c is the lattice constant of the supercell. From the cross-sectional view, six edges of the hexagon cut the Zn–O bonds through
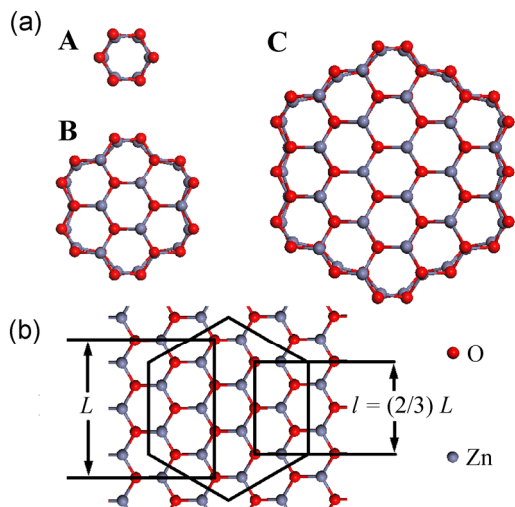
Figure 1 (a) Cross-sections of relaxed ZnO nanowires of different sizes. (b) Schematic illustrating the method used to estimate the cross-sectional area of nanowire B. The cross-sectional area is specified by the hexagon with the black edge, and the lengths L and l are indicated in the figure.

the middle, which correctly accounts for the volume. Therefore, the S value for the nanowire can be obtained by determining the area of the black regular hexagon, as shown in Fig. 1(b). The longest length, L, within the supercell along the a-axis can be used to calculate the edge length of the hexagon, l.

$$l = (n/(2n-1))/L \qquad (3)$$

where n is the shell number of a nanowire. Thus the nanowire's volume per supercell can be presented as

$$V = Sc = \left(3\sqrt{3}/2\right)l^2 c = \left(3\sqrt{3}/2\right)\left(n/(2n-1)\right)^2 L^2 c \qquad (4)$$

This formula can also be used to calculate the volume of relaxed ZnO nanowires. Since Zn atoms move inward much more readily than O atoms after geometry relaxation, the length L should be treated as the average value of Zn and O atoms. Another volume calculation method, which considers atoms as point charges, is illustrated in Fig. S1 (in the Electronic Supplementary Material (ESM)). Because electrons occupy most of the space in the material, it is unreasonable to treat atoms as point charges in the surface region. Doing so will undervalue the volume of a nanowire, especially for nanowire A, as shown in Fig. S2 in the ESM. Therefore, we used the calculation method illustrated in Fig. 1(b).

3 Results and discussion

The calculated structural parameters and the piezo-electric coefficient, e_{33}, for ZnO bulk are shown in Table 1. The structural parameters are in good agreement with the experimental values [25], and e_{33} is close to that reported in a previous work [14]. These results show that our modeling approach and pseudopotentials for ZnO structures and piezoelectric properties are valid.

Geometry relaxation was performed for the ZnO nanowires without any strain, and the structural parameters are listed in Table 2. It is clear that lattice constant c increases and the volume per Zn–O pair decreases with decreasing nanowire diameter. The surface atom displacement can be seen in Fig. 1(a), whereas atoms in the core region remain essentially stationary. The lateral size of the nanowire obviously contracts because L is smaller than L_0 in Table 2; the energy of the nanowire is higher than that of bulk, as revealed in Li et al.'s work [16]. To calculate the effective piezoelectric coefficients, e_{33}^{eff}, of the ZnO nanowires, a series of strains from –1% to 1% in increments of 0.2% were applied along the c-axis. The atomic coordinates were fully relaxed, and thus the lateral size of the nanowires changes during the strain. It should be noted that one should not compare the nanowire e_{33}^{eff} to the bulk e_{33} in evaluating the size effects. Also, the lateral contraction or expansion

**Table 1** Structural parameters and piezoelectric coefficient, e_{33}, of ZnO bulk

	a (Å)	c (Å)	u	e_{33} (C·m^{-2})
This work	3.249	5.220	0.380	1.26
Reference	3.249 [25]	5.205 [25]	0.382 [25]	1.28 [14]

Table 2 The structure details for the relaxed ZnO nanowires: unrelaxed lateral length (L_0), relaxed lateral length (L), relaxed lattice constant (c), average volume (V_a), fractional coordinate (u), surface atom ratio (η), and Poisson's ratio (v)

Sample	L_0 (Å)	L (Å)	V_a (Å^3)	c (Å)	u	η	v
A	3.249	2.979	20.648	5.375	0.341	1.00	0.474
B	9.747	9.201	21.600	5.302	0.345	0.75	0.412
C	16.245	15.685	22.454	5.269	0.358	0.56	0.376
Bulk			23.861	5.220	0.380	0.00	0.337

during the strain must be taken into account when calculating the bulk e_{33}^{eff}. Therefore, a Poisson's ratio of 0.337 for ZnO bulk was implemented as calculated in our previous work [26].

The macroscopic polarization along the [0001] direction was calculated and plotted in Fig. 2. The figure clearly reveals that at a given strain, the P_3 value of any nanowire is significantly larger than that of ZnO bulk, and a good linear correlation between P_3 and the strain can be found. Here the macroscopic polarization is different from the conventional net polarization, which is relative to a reference system. But the macroscopic value is more general and brief, and so we use it to clearly characterize the polarization of ZnO nanowires. The linear regression method was employed to obtain slopes for nanowires A, B, and C and the ZnO bulk, and the slope is just right the e_{33}^{eff}, as defined in Eq. (1). We list the obtained coefficients in Table 3, together with those from some previous works. In the third column, we have transformed the unit of effective piezoelectric coefficient into C·m^{-2} in Xiang et al.'s work [17] through our volume calculation methods in the paper's second section.
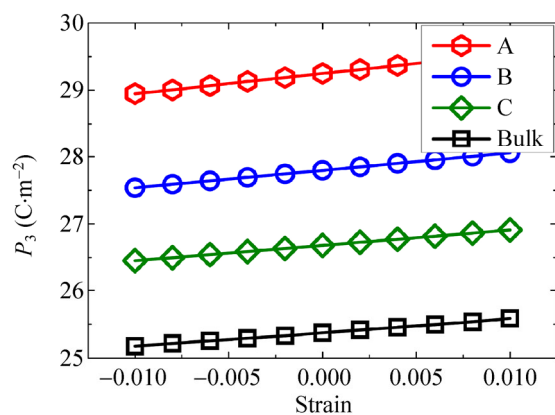
Figure 2 Macroscopic polarization along the *c*-axis as a function of strain for relaxed ZnO nanowires and the bulk.

Table 3 The effective piezoelectric coefficient (C·m^{-2}) for different ZnO structures in the current work and references

| Sample	This work	Ref. [17]	Ref. [18]	Ref. [27]
A	29.985	28.167	119.94	
B	25.756	25.552	45.789	7.995
C	22.735	26.137	32.739	4.376
Bulk	20.189	20.211	19.210	1.880

The size effects here are similar to the results converted from Xiang's work [17] but obviously not as large as those reported by Agrawal and Espinosa [18]. The large deviation can be attributed to the methods (illustrated in Fig. S1 in the ESM) used to evaluate the volume of ZnO nanowires. In Hoang et al.'s [27] definition for effective piezoelectric coefficient, the volume was fixed, and thus they obtained relatively low values. In our work, the difference of e_{33}^{eff} between nanowire C and the bulk is not very large.

Previous works [17, 18, 27] also reported the size effects of piezoelectric properties but without further explanation. In order to make the comparison between different structures meaningful, the average macroscopic electric dipole moment, p_{3a}, and the average volume per Zn–O pair, V_a, were used. Equation (1) can thus be written as

$$
\begin{aligned}
e_{33}^{\text{eff}} &= \partial(p_3 / V) / \partial\epsilon_3 = \partial(p_{3a} / V_a) / \partial\epsilon_3 \\
&= (\partial p_{3a} / \partial\epsilon_3)V_a^{-1} + p_{3a}(\partial V_a^{-1} / \partial\epsilon_3)
\end{aligned}
\tag{5}
$$

Thus both p_{3a} and the reciprocal of average volume, V_a^{-1}, as a function of strain determine the effective piezoelectric coefficient, and they are plotted as functions of strain in Fig. 3. It is clear that p_{3a} increases with increasing strain, whereas it decreases with increasing diameter; on the other hand, V_a^{-1} decreases with increasing strain and diameter. However, the bulk value of p_{3a} is larger than that of any nanowire, which was found in a previous work [18].

In order to understand how p_{3a} and V_a^{-1} influence the effective piezoelectric coefficients, the numerical results of the variables in Eq. (5) are listed in Table 4. It can be seen clearly that both p_{3a} and $\partial p_{3a} / \partial\epsilon_3$ change only slightly as a function of the size of the nanowires, whereas V_a^{-1} and $\partial V_a^{-1} / \partial\epsilon_3$ change significantly. The first term, $(\partial p_{3a} / \partial\epsilon_3)V_a^{-1}$, changes from 31.429 C·m^{-2} for nanowire A to 26.792 C·m^{-2} for the bulk; the second term, $p_{3a}(\partial V_a^{-1} / \partial\epsilon_3)$, changes from −1.441 C·m^{-2} for nanowire A to −6.605 C·m^{-2} for the bulk. In previous works, it was seen that the volume reduction of a nanowire enhances e_{33}^{eff} with respect to the bulk crystal. Fig. S2 in the ESM reveals that the use of an unreasonable method for volume calculation led to very large effective piezoelectric coefficients, especially for nanowire A. This method, which led to remarkably small average volumes for thin nanowires,
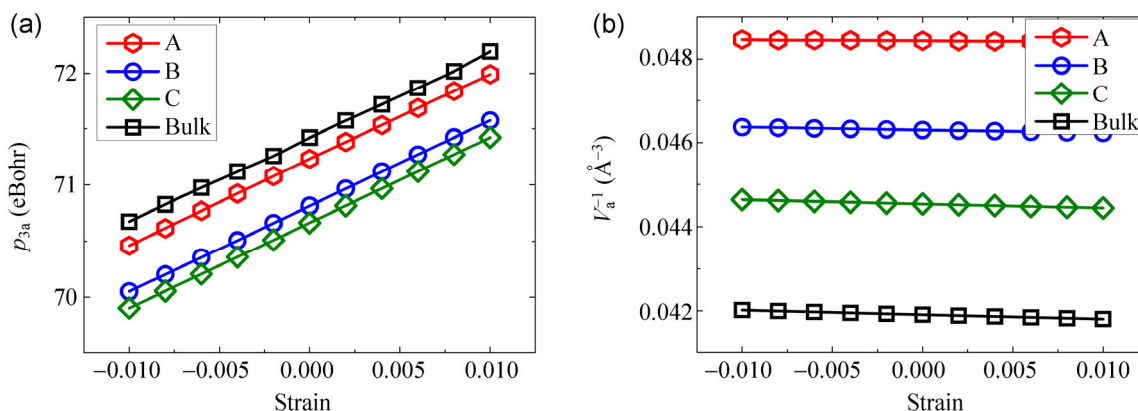
Figure 3 (a) p_{3a} as a function of strain for relaxed ZnO nanowires. (b) V_a^{-1} as a function of strain for relaxed ZnO nanowires.

Table 4 The value of variables in Eq. (5) for ZnO nanowires and bulk

Sample	$\partial p_{3a}/\partial \epsilon_3$ (eBohr)	V_a^{-1} (Å^{-3})	$(\partial p_{3a}/\partial \epsilon_3)V_a^{-1}$ (C·m^{-2})	p_{3a} (eBohr)	$\partial V_a^{-1}/\partial \epsilon_3$ (Å^{-3})	$p_{3a}(\partial V_a^{-1}/\partial \epsilon_3)$ (C·m^{-2})	e_{33}^{eff} (C·m^{-2})
A	76.544	0.04843	31.429	71.231	−0.00239	−1.441	29.986
B	76.307	0.04587	29.674	70.812	−0.00665	−3.993	25.752
C	76.031	0.04412	28.437	70.662	−0.00974	−5.833	22.733
Bulk	75.389	0.04191	26.792	71.421	−0.01090	−6.605	20.187

resulted in obtained coefficients in Agrawal and Espinosa's work [18] that were very large. Furthermore, this current work demonstrates that the change of average volume during the strain reduces the e_{33}^{eff} value. Ignoring the change of volume will surely underestimate the coefficients, as in Hoang et al.'s work [27]. Therefore, both the reduction of average volume and the change of average volume with strain play almost equally important roles in terms of the size effects of piezoelectricity.

A very brief modulus determining the term $\partial V_a^{-1}/\partial \epsilon_3$ is Poisson's ratio v. A higher v means a higher $\partial V_a^{-1}/\partial \epsilon_3$, which is clearly found in the data in Tables 2 and 4. Therefore, it is noteworthy that recent works have shown extensively dispersed Poisson's ratios for various ZnO materials. Pant et al. [28] characterized the structure of epitaxial ZnO films through a two-step growth method at various low temperatures, which leads to abnormal Poisson's ratios ranging from 0.08 to 0.54. For single-walled ZnO nanotubes, Mirnezhad et al. [29] demonstrated changing values from 0.2 to 0.61 with different patterns of hydrogen adsorption. Qing et al. [30] also obtained a high Poisson's ratio of

0.667 for a graphene- like hexagonal ZnO monolayer. Therefore, attention to Poisson's ratio may be helpful for piezoelectricity investigation in ZnO nanomaterials.

After studying the size dependence of piezoelectricity for ZnO nanowires, we further studied the polarization mechanism of ZnO nanowires along the [0001] direction. The change in average macroscopic dipole moment can be related to three major factors: (i) the lattice constant, c, (ii) the fractional coordinate, u, and (iii) the ratio of surface atoms, η. The above parameters were calculated and are listed in Table 2. Therefore, the average dipole moment p_{3a} may be expressed as

$$p_{3a} = f(c,u) + h_{\text{Surf}}(\eta) + p_{3a}^0 \qquad (6)$$

where $f(c,u)$ and $h_{\text{Surf}}(\eta)$ account for the contributions of crystal structure and surface effect, respectively, and p_{3a}^0 is a constant value.

In order to study the effect of each parameter, further DFT calculations were performed on unrelaxed nanowires with different values of c and u. Values of p_{3a} as functions of c and u are plotted in Figs. 4(a) and 4(b), respectively. It was found that increasing c or
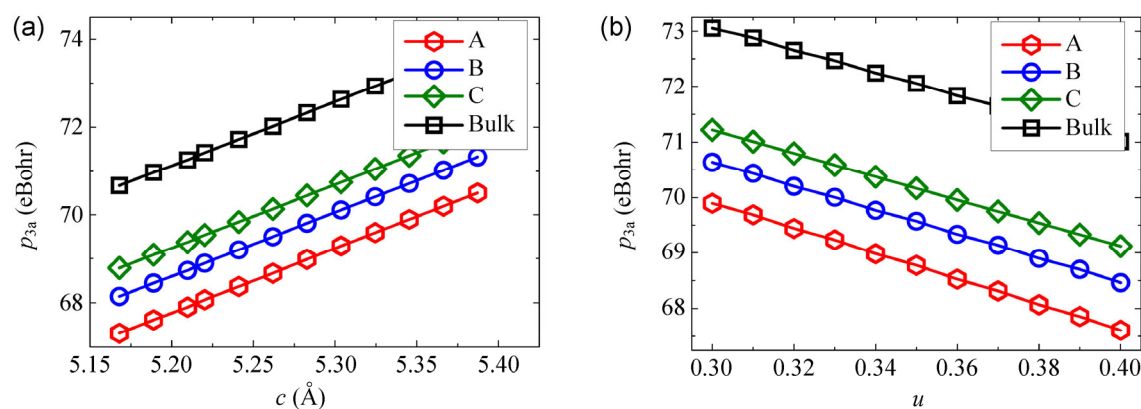
Figure 4 (a) Averaged macroscopic electric dipole moment as a function of lattice constant c for unrelaxed ZnO nanowires and the bulk. (b) Averaged macroscopic electric dipole moment as a function of fractional coordinate u for unrelaxed ZnO nanowires and the bulk.

decreasing u can lead to a higher p_{3a} values, and Fig. 4 demonstrates very good linear correlations between p_{3a} and c and between p_{3a} and u for ZnO nanowires. The slopes for each set of data in Fig. 4 were evaluated and are listed in Table 5. The values of $\partial p_{3a} / \partial c$ for different nanowires, in other words, for different surface atom ratios, are almost the same, which supports our decision to split the contributions of structure relaxation and surface ratio in Eq. (6). Therefore, we chose $\partial p_{3a}(c, u, \eta) / \partial c = \partial f(c, u) / \partial c = I_c = 14.60$ eBohr to evaluate the contribution of c. Similarly, we have $\partial p_{3a}(c, u, \eta) / \partial u = \partial f(c, u) / \partial u = I_u = -22.89$ eBohr. From the above results, we can make the following statement about the effect of structure on the polarization of ZnO: Large c or small u will lead to large p_{3a} with a linear correlation.

To understand the underlying physics, let us discuss the subject further. Since the value of the macroscopic electric dipole moment can be simply obtained as the product of charge and distance between the ions, it is easily found that the enhancement of c will surely increase p_{3a}. As a simple example, assume a linear relationship between p_{3a} and c; thus $\partial p_{3a} / \partial c \approx p_{3a} / c$. The estimated p_{3a}/c values are also listed in Table 5 after the $\partial p_{3a} / \partial c$ column for easy comparison. It can be seen that the values in the two columns are close and that the deviation is somewhat larger for ZnO nanowire A. This indicates that the effect of c on p_{3a} is mainly attributed to the displacement of ions in the unit cell.

At the same time, increasing u means that the O atom plane moves closer to the Zn atom plane, so that the polarization along the c direction is weakened, which reduces p_{3a}. As a simple example, O and Zn ions assume a formal charge q (2e for Zn and –2e for O ions), and the displacement of the ion center can be estimated as –($c \times \partial u$). Therefore, the change in p_{3a} with u can be calculated according to $\partial p_{3a}/\partial u \approx -(q \times c)$. The $\partial p_{3a}/\partial u$ values calculated from first-principle calculations and the estimated –($q \times c$) values are listed in Table 5 for comparison. One should note that the unrelaxed structures share the same c and thus the same –($q \times c$). It can be seen that the values of $\partial p_{3a}/\partial u$ and –($q \times c$) are quite close. This is why the macroscopic dipole moment is a very general quantity in condensed matter, and we should pay more attention to it.

For the fully relaxed nanowires, which show higher values of c and lower values of u than the bulk ZnO (which can be found in Table 2), the relaxed crystal structure leads to higher values of p_{3a} than the unrelaxed ones. Therefore, the structure relaxation is to some extent compensation for polarization reduction.

Table 5 Values of p_{3a}, $\partial p_{3a}/\partial c$, p_{3a}/c, $\partial p_{3a}/\partial u$ and $-qc$ for the unrelaxed ZnO nanowires and bulk

| Sample	p_{3a} (eBohr)	$\partial p_{3a}/\partial c$ (eBohr/Å)	p_{3a}/c (eBohr/Å)	$\partial p_{3a}/\partial u$ (eBohr)	$-qc$ (eBohr)
A	68.068	14.60	12.66	–22.89	–20.32
B	68.898	14.55	12.99	–21.77	–20.05
C	69.538	14.50	13.20	–21.02	–19.92
Bulk	71.421	14.45	13.68	–20.49	–19.74

In order to study the surface effect, the average macroscopic dipole moment along the c-axis (p_{3a}) as a function of surface ratio (η) for relaxed and unrelaxed ZnO nanowires and the bulk without strain are plotted in Fig. 5. A linear correlation between the p_{3a} and η can be seen clearly for the unrelaxed ZnO nanowires. As the nanowire grows thicker, the surface atom ratio decreases and p_{3a} increases. Therefore, we have

$$h_{\text{Surf}}\left(\eta\right) = \gamma_S \eta \qquad (7)$$

where γ_S is a constant value ($\gamma_S = -3.353$ eBohr). Therefore, the average dipole moment of the unrelaxed nanowire is linearly dependent on the surface atom ratio. From the negative value of γ_S, it can be concluded that surface atoms contribute less than the core atoms. This is due to the redistribution of charge among the core and surface ions, and the dangling bonds at the surface impair the polarization behavior. Thus the corresponding average dipole moment of every Zn–O pair at the surface is lower than that of the core region or bulk. An explanation as to why the average dipole moment for nanowires is smaller than that of bulk was also presented in Agrawal and Espinosa's work [18] in terms of Mulliken charges. They found that the surface of a Zn–O pair shows a noticeable decrease of dipole moment with respect to the bulk value. Moreover, Hoang et al.'s work [27] also revealed that the surface will significantly impair the piezoelectric behavior along the c-axis through the continuum slab model. Finally, the average macroscopic dipole moment, p_{3a}, can be written as

$$p_{3a}(c, u, \eta) = I_c(c - c_0) + I_u(u - u_0) + \gamma_S \eta + p_{3a}^0 \qquad (8)$$

It is clear that p_{3a}^0 represents the average macroscopic dipole moment of the bulk, which shows no surface atom ratio ($\eta = 0$). For a fully relaxed nanowire, Eq. (8) can be used to evaluate p_{3a} with crystal structure parameters and surface ratios. The blue triangles in Fig. 5 represent the DFT-calculated results, whereas the light-blue curve shows the results of Eq. (8); there is a good match between the two sets of data. A good match also shows that the average macroscopic dipole moment along the [0001] direction is only minimally influenced by lateral structural relaxation, which is
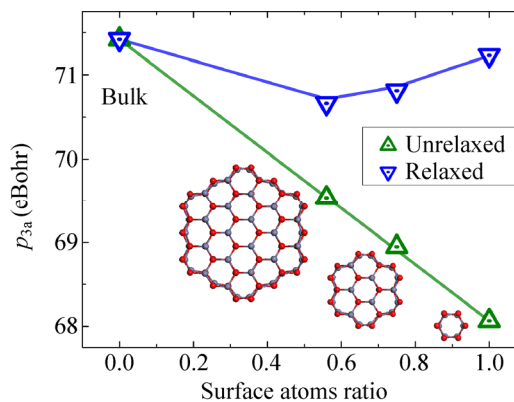
Figure 5 Average macroscopic electric dipole moment along the c-axis as a function of surface ratio for relaxed and unrelaxed ZnO nanowires and the bulk without strain. The light green and blue curves are the linear and formula fits of the unrelaxed and relaxed nanowires, respectively.

not included in Eq. (8). The surface atom ratios of experimentally prepared ZnO nanowires are very close to 0, but the nanowires may have different observable structure parameters due to various conditions. Thus the above representation allows us to possibly extrapolate the macroscopic polarization in ZnO nanostructures.

4 Conclusion

First-principles calculations were carried out to study the piezoelectric and polarization features of ZnO nanowires along the c-axis and their size effects. The effective piezoelectric coefficients of nanowires are larger than the bulk value, and the coefficient values increase significantly as the nanowire diameter decreases. In particular, explanations for piezoelectric size effects have been discussed, and both the average volume per Zn–O pair in nanowires and the volume change rate with strain play key roles. Furthermore, theoretical predictions indicate that the polarization behavior of ZnO nanowires mainly depends on two contributions, one related to the crystal parameters (including lattice constant c and fractional coordinate u) and the other to the surface atom ratios. Also, an analytical expression to describe the macroscopic average dipole moment was obtained using structural variables. Our work establishes an integrated methodology for investigating piezoelectricity and polarization properties in ZnO nanowires, and these

methods can be used to predict the piezoelectricity and polarization properties of wurtzite-structured nanowires such as GaN, AlN, etc.

Acknowledgements

Electronic Supplementary Material: Supplementary material (the method for volume calculation considering atoms as point charges) is available in the online version of this article at http://dx.dio.org/10.1007/s12274-015-0718-x.

References

[1] Zhang, Y.; Yan, X. Q.; Yang, Y.; Huang, Y. H.; Liao, Q. L.; Qi, J. J. Scanning probe study on the piezotronic effect in ZnO nanomaterials and nanodevices. *Adv. Mater.* **2012**, *24*, 4647–4655.

[2] Zhang, Z.; Liao, Q. L.; Yan, X. Q.; Wang, Z. L.; Wang, W. D.; Sun, X.; Lim, P.; Huang, Y. H.; Zhang, Y. Functional nanogenerators as vibration sensors enhanced by piezotronic effects. *Nano Res.* **2014**, *7*, 190–198.

[3] Liao, Q. L.; Zhang, Z.; Zhang, X. H.; Mohr, M.; Zhang, Y.; Fecht, H.-J. Flexible piezoelectric nanogenerators based on a fiber/ZnO nanowires/paper hybrid structure for energy harvesting. *Nano Res.* **2014**, *7*, 917–928.

[4] Wang, X. D.; Song, J. H.; Liu, J.; Wang, Z. L. Direct-current nanogenerator driven by ultrasonic waves. *Science* **2007**, *316*, 102–105.

[5] Lin, P.; Chen, X.; Yan, X. Q.; Zhang, Z.; Yuan, H. G.; Li, P. F.; Zhao, Y. G.; Zhang, Y. Enhanced photoresponse of Cu_2O/ZnO heterojunction with piezo-modulated interface engineering. *Nano Res.* **2014**, *7*, 860–868.

[6] Wang, Z. L. Piezopotential gated nanowire devices: Piezotronics and piezo-phototronics. *Nano Today* **2010**, *5*, 540–552.

[7] Yu, R. M.; Pan, C. F.; Hu, Y. F.; Li, L.; Liu, H. F.; Liu, W. Chua, S.; Chi, D. Z.; Wang, Z. L. Enhanced performance of GaN nanobelt-based photodetectors by means of piezotronic effects. *Nano Res.* **2013**, *6*, 758–766.

[8] Liu, B.; Zeng, H. C. Direct growth of enclosed ZnO nanotubes. *Nano Res.* **2009**, *2*, 201–209.

[9] Yin, X.; Wang, B.; He, M.; He, T. Facile synthesis of ZnO nanocrystals via a solid state reaction for high performance plastic dye-sensitized solar cell. *Nano Res.* **2012**, *5*, 1–10.

[10] Li, P. F.; Liao, Q. L.; Yang, S. Z.; Bai, X. D.; Huang, Y. H.; Yan, X. Q.; Zhang, Z.; Liu, S.; Lin, P.; Kang, Z., et al. *In situ* transmission electron microscopy investigation on fatigue behavior of single ZnO wires under high-cycle strain. *Nano Lett.* **2014**, *14*, 480–485.

[11] Son, D. I.; Kwon, B.W.; Yang, J. D.; Park, D. H.; Seo, W. S.; Lee, H.; Yi, Y.; Lee, C. L.; Chio, W. K. Charge separation and ultraviolet photovoltaic conversion of ZnO quantum dots conjugated with graphene nanoshell. *Nano Res.* **2012**, *5*, 747–761.

[12] Hu, G. F.; Zhou, R. R.; Yu, R. M.; Dong, L.; Pan, C. F.; Wang, Z. L. Piezotronic effect enhanced Schottky-contact ZnO micro/nanowire humidity sensors. *Nano Res.* **2014**, *7*, 1083–1091.

[13] Xu, F.; Qin, Q. Q.; Mishra, A.; Gu, Y.; Zhu, Y. Mechanical properties of ZnO nanowires under different loading modes. *Nano Res.* **2010**, *3*, 271–280.

[14] Wu, X. F.; Vanderbilt, D.; Hamann, D. R. Systematic treatment of displacements, strains, and electric fields in density-functional perturbation theory. *Phys. Rev. B* **2005**, *72*, 035105.

[15] Noel, Y.; Llunell, M.; Orlando, R.; D'Arco, P.; Dovesi, R. Performance of various Hamiltonians in the study of the piezoelectric properties of crystalline compounds: The case of BeO and ZnO. *Phys. Rev. B*, **2002**, *66*, 214107.

[16] Li, C.; Guo W. L.; Kong Y.; Gao H. J. First-principles study of the dependence of ground-state structural properties on the dimensionality and size of ZnO nanostructures. *Phys. Rev. B*, **2007**, *76*, 035322.

[17] Xiang, H. J.; Yang, J. L.; Hou, J. G.; Zhu, Q. S. Piezoelectricity in ZnO nanowires: A first-principles study. *Appl. Phys. Lett.* **2006**, *89*, 223111.

[18] Agrawal, R.; Espinosa, H. D. Giant piezoelectric size effects in zinc oxide and gallium nitride nanowires. A first principles investigation. *Nano Lett.* **2011**, *11*, 786–790.

[19] Cicero, G.; Ferretti, A.; Catellani, A. Surface-induced polarity inversion in ZnO nanowires. *Phys. Rev. B* **2009**, *80*, 201304.

[20] Korir, K. K.; Cicero, G.; Catellani, A. Piezoelectric properties of zinc oxide nanowires: An ab initio study. *Nanotechnology* **2013**, *24*, 475401.

[21] Soler, J. M.; Artacho, E.; Gale, J. D.; Garcia, A.; Junquera, J.; Ordejón, P.; Sánchez-Portal, D. The SIESTA method for *ab initio* order-N materials simulation. *J. Phys.*: *Condens. Matter* **2002**, *14*, 2745–2779.

[22] Troullier, N.; Martins, J. L. Efficient pseudopotentials for plane-wave calculations. *Phys. Rev. B* **1991**, *43*, 1993–2006.

[23] King-Smith, R. D.; Vanderbilt, D. Theory of polarization of crystalline solids. *Phys. Rev. B* **1993**, *47*, 1651–1654.

[24] Resta, R. Macroscopic polarization in crystalline dielectrics: The geometric phase approach. *Rev. Mod. Phys.* **1994**, *66*, 899–915.

[25] Yoshio, K.; Onodera, A.; Satoh, H.; Sakagami, N.; Yamashita, H. Crystal structure of ZnO:Li at 293 K and 19 K by X-ray diffraction. *Ferroelectrics* **2001**, *264*, 133–138.

[26] Huang, Y. H.; Zhang, Y.; Wang, X. Q.; Bai, X. D.; Gu, Y. S.; Yan, X. Q.; Liao, Q. L.; Qi, J. J.; Liu, J. Size independence and doping dependence of bending modulus in ZnO nanowires. *Cryst. Growth Des.* **2009**, *9*, 1640–1642.

[27] Hoang, M. T.; Yvonnet, J.; Mitrushchenkov, A.; Chambaud, G. First-principles based multiscale model of piezoelectric nanowires with surface effects. *J. Appl. Phys.* **2013**, *113*, 104309.

[28] Pant, P.; Budai, J. D.; Aggarwal, R.; Narayan, R. J.; Narayan, J. Structure characterization of two-step growth of epitaxial ZnO films on sapphire substrates at low temperatures. *J. Phys. D*: *Appl. Phys.* **2009**, *42*, 105409.

[29] Mirnezhad, M.; Ansari, R.; Rouhi, H. Effects of hydrogen adsorption on mechanical properties of chiral single walled zinc oxide nanotubes. *J. Appl. Phys.* **2012**, *111*, 04308.

[30] Peng, Q.; Liang, C.; Ji, W.; De, S. A first principles investigation of the mechanical properties of g-ZnO: The graphene-like hexagonal zinc oxide monolayer. *Comp. Mater. Sci.* **2013**, *68*, 320–324.